



A Model to Determine the Advective Circulation in a Three Layer, Salt Wedge Estuary: Application to the Ebre River Estuary

C. Ibàñez^a, J. Saldaña^b and N. Prat^a

^aDepartament d'Ecologia, Universitat de Barcelona, Av. Diagonal 645, 08028 Barcelona, Spain

^bDepartament de Matemàtica i Informàtica, Universitat de Vic, c. Sagrada Família 7, 08500 Vic, Barcelona, Spain

A model to determine advective fluxes of water and salt in three-layer salt wedge estuaries under steady river discharge is presented. This model is a generalization of the Knudsen's two-layer model when applied to highly stratified estuaries. The reason for this is that Knudsen's model neglects the interface and produces biased estimates of the salt fluxes at this layer. A basic assumption of the model is that velocity and salinity have linear profiles across the interface, which is appropriate for such types of estuaries. A physical description of the Ebre estuary is given in terms of river discharge, mean salinity in upper and lower layers, and cross-sectional area of all three layers. These data are introduced into the model in order to obtain estimates of horizontal and vertical fluxes. The equations for horizontal fluxes are: the steady salt and water transport conditions at any cross-section and a flow relation between the three layers. Solving the three mentioned equations, explicit expressions for horizontal fluxes are obtained. Introducing the latter in the salt and water continuity equations of upper and lower layers, vertical fluxes of water and salt at any given compartment along the estuary are obtained. These vertical fluxes among the three layers allow more precise information to be obtained about mixing processes within the estuary. A comparison of the results with those corresponding to the Knudsen's two-layer model shows that the model gives a more accurate estimate of advective fluxes in highly stratified estuaries.

© 1999 Academic Press

Keywords: salt wedge estuary; advective circulation; three-layer model; box model

Introduction

A salt wedge occurs in an estuary when the river discharge is adequate enough to maintain a strong gradient between fresh and salt water against the mixing tendency of tide and wind-induced turbulence (Geyer & Farmer, 1989). Salt wedge estuaries occur at the last reach of rivers flowing into the sea with a low tidal range, though they can be present in high tidal areas when the ratio of river discharge to the width of the estuary is high. Research concerning salt wedge estuaries has been scarce and focused on hydrological aspects (Keulegan, 1966; Wright & Coleman, 1971; Rattray & Mitsuda, 1974; Geyer & Smith, 1987; Partch & Smith, 1987; Geyer & Farmer, 1989). Studies concerning circulation and mixing in salt wedge estuaries with high tidal range focus on the time dependent dynamics because tidal dynamics are more important than non-tidal dynamics. With a low tide range, advective circulation can prevail over tidal circulation and the advance or retreat of a salt wedge depends largely on river discharge, although the topography of the bottom is also a determinant factor (Ibàñez *et al.*, 1995, 1997), as well as the tide in the zone near the mouth (Guillén, 1992). In the Ebre coast (NW Mediterranean), the tidal range is small

(20 cm). With steady river flow, the advance or retreat of the salt wedge eventually ceases, and the still form is called an arrested saline wedge (Keulegan, 1966). The authors present a three layer model (upper, lower and interface layers) to predict advective salt and water fluxes in salt wedge estuaries as a function of river discharge and salinity distribution, for any single case.

The model is an improvement of the Knudsen's two-layer model when applied to highly stratified estuaries. Both are based on the salt balance equation and are only valid for estuaries where the salt flux is basically advective. However, Knudsen's model neglects the interface layer, and this produces incorrect estimates of the salt flux at this layer. The reason is that the existence of strong gradients of salinity and velocity with opposite slopes in this layer does not allow a correct estimate of the salt flux by multiplying the mean flow by the mean salinity. Here this situation is overcome by considering the interface as a distinct layer.

Site description and methods

The Ebre river is 928 km long, and its mean annual discharge is $424 \text{ m}^3 \text{ s}^{-1}$. The Ebre Delta (see Figure 1) is located at $40^\circ 40'$ latitude and $0^\circ 40'$ longitude. It

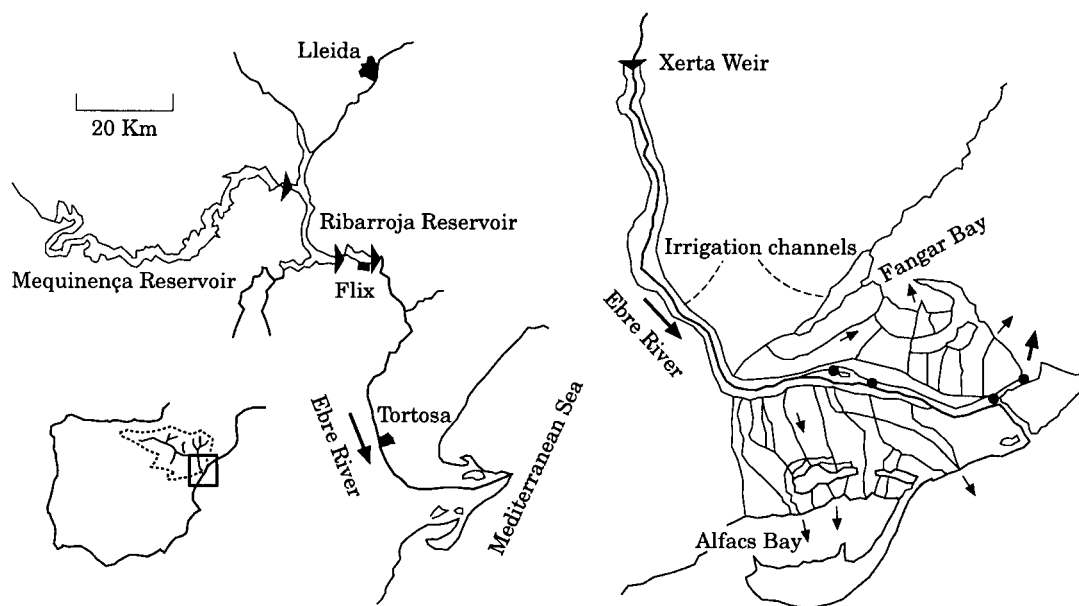


FIGURE 1. Geographical description of the Ebre Delta.

has an area of 330 km² and the deltaic reach of the river is 29 km long, with a mean maximum depth value of 6.8 m and a mean width of 237 m at the river surface. The maximum length of the salt wedge is about 32 km.

Several surveys along the Ebre river estuary were carried out from April 1988 to July 1992, within a 4 year research programme to study the hydrological dynamics and ecological functioning of this estuarine system (Ibáñez, 1993). Detailed profiles of salinity, temperature, velocity and dissolved oxygen were made every 2 or 3 km, over the whole water column. The surveys were carried out during low river discharge as this is when the salt wedge is present in the Ebre estuary. The data used in this paper correspond to salinity and velocity profiles, and were obtained by means of a WTW LF 191 conductivitymeter with automatic temperature compensation and a Valeport Brystoke BFM001 currentmeter, respectively.

To determine advective fluxes between the three layers along the estuary, a detailed survey of salinity profiles (every 20 cm over the whole water column) was carried out every 2 km on 13 March 1989. The river discharge was 60 m³ s⁻¹ and the salt wedge extended 30 km upstream from the mouth, which allowed the authors to divide the estuary into 15 compartments.

The model

The aim of this section is to develop a three-layer model equivalent to Knudsen's model, because the neglect of an intermediate layer (the interface) in

highly stratified estuaries causes biased estimates of the advective fluxes. Figure 2 shows typical profiles of salinity, velocity and longitudinal salt transport through the water column in the Ebre estuary. As can be seen, the velocity and salinity profiles are linear across the interface, but with opposite slope. As a result, the salt transport profile is not linear, showing a maximum at the middle of the layer. This implies that the salt transport at the interface cannot be correctly determined by multiplying the mean water flow by the mean salinity of the layer. This problem arises when the Knudsen's two-layer model is applied to highly stratified estuaries, because in such a model the interface is not considered as a different layer. It is important to take into account that, in this type of estuary, the salt transport at the interface is a relevant part of the total salt transport to the sea, representing between 30 and 50% in the case of the Ebre estuary.

Considering the previous statements, the question is: what to do with the interface when the Knudsen's two-layer model is applied to a highly stratified estuary? The interface should be incorporated to the upper layer because both layers flow in the same direction. The reason is that the mean water velocities in the upper (riverine) layer are usually an order of magnitude higher than in the lower layer. In this situation, the Knudsen's model always produces an overestimation of the advective fluxes of salt and water (see further explanations). Thus, it is convenient to construct a three-layer model equivalent to the two-layer Knudsen model, in order to solve the problem of the interface in highly stratified estuaries.

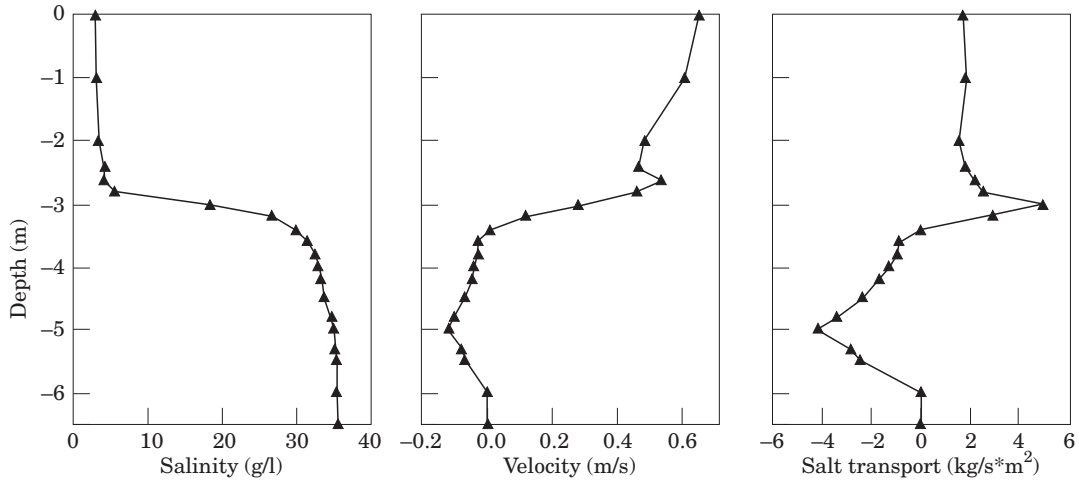


FIGURE 2. Typical salinity, velocity and salt transport profiles in the Ebre estuary. Notice the maximum of salt transport at the middle of the interface.

For this type of estuary, the assumption that the velocity and salinity have linear profiles across the interface is appropriate (Geyer & Smith, 1987). Under such assumption, we can introduce flow, salinity and salt flux in this layer with knowledge only of the upper and lower layer conditions. In particular, if a constant width (w_2) across the interface is assumed, the salt flux at the interface is

$$f_s = w_2 \int_0^\delta u_2(z) s_2(z) dz \quad (1)$$

where δ is the thickness, u_2 and s_2 are the velocity and salinity at the interface layer, respectively. Now, under the hypothesis of linearity of the gradients, s_2 and u_2 can be obtained in terms of the salinities s_i and velocities u_i of the upper and lower layer ($i=1, 3$, respectively), namely,

$$s_2(z) = s_1 + \frac{(s_3 - s_1)}{\delta} z, \quad u_2(z) = u_1 + \frac{(u_3 - u_1)}{\delta} z. \quad (2)$$

Substituting (2) into (1) and integrating, the salt flux at the interface is given by

$$f_s(u_1, u_3) = \frac{1}{3} a_2 \left[u_1 \left(s_1 + \frac{s_3}{2} \right) + u_3 \left(s_3 + \frac{s_1}{2} \right) \right] \quad (3)$$

where $a_2 = w_2 \delta$ is the cross sectional area of the interface.

For convenience, let us express the salt flux at the interface given by (3) in terms of water flows, namely,

$$f_s(q_1, q_3) = \frac{1}{3} a_2 \left[\frac{q_1}{a_1} \left(s_1 + \frac{s_3}{2} \right) + \frac{q_3}{a_3} \left(s_3 + \frac{s_1}{2} \right) \right] \quad (4)$$

where $q_i = a_i u_i$ is the water flow of the upper and lower layers ($i=1, 3$, respectively) with a_i the cross sectional area of the i -layer.

In principle, this derivation of the salt flux at the interface neglects changes of water levels in time. This is suitable for salt-wedge estuaries, which are basically associated with microtidal seas (e.g. the Mediterranean and the Gulf of Mexico), where time-dependent models are not needed to describe the circulation pattern of the estuary (see Ibañez *et al.*, 1997). However, Equation (4) remains true if tidal oscillations are considered, as long as the three-layer structure and the linear profiles of salinity and velocity across the interface persist (which is usually the case) but, now, f_s becomes a function of time.

Assuming constant profiles of u_1 , u_3 , s_1 and s_3 , a constant width for each layer and no change in water levels, the system of equations of the model to determine horizontal fluxes of water and salt of the three layers at any point in the estuary are:

$$q_1 s_1 + f_s(q_1, q_3) + q_3 s_3 = 0 \quad (5)$$

$$q_1 + q_2 + q_3 = R \quad (6)$$

$$\frac{q_1}{a_1} - 2 \frac{q_2}{a_2} + \frac{q_3}{a_3} = 0 \quad (7)$$

where, for each layer, a_i is the cross sectional area, $q_i = a_i u_i$ is the water flow and s_i is the salinity (the subscript $i=1, 2, 3$ refers to upper, interface and lower layer, respectively), $f_s(q_1, q_3)$ is the salt flux at the interface given by (4) and R is the river flow entering the estuary.

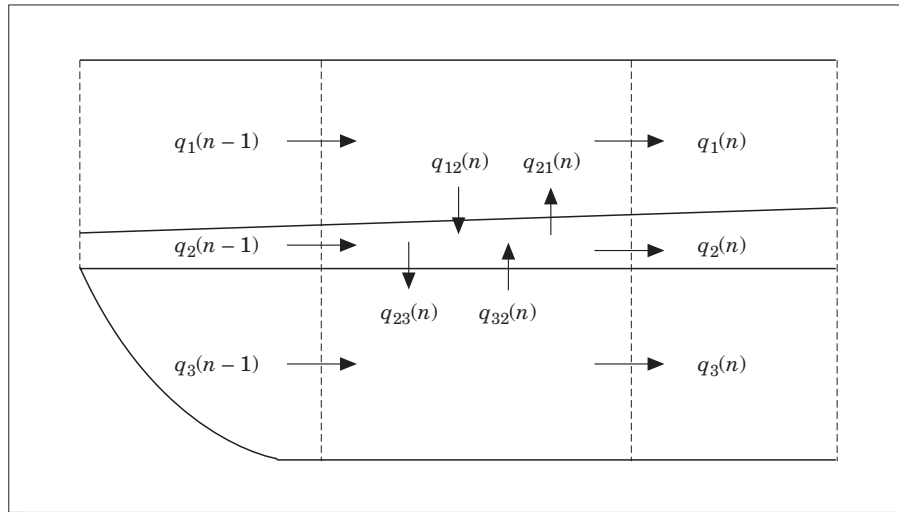


FIGURE 3. Diagram of the estuary showing the three layers and some compartments, with the notations of the equations.

Equations (5) and (6) are the steady salt and water transport conditions at any cross section of the estuary, whereas Equation (7) is the flow relation between the three layers based on the assumption of linearity of the velocity profile at the interface. More precisely, this assumption implies that

$$q_2 = w_2 \int_0^\delta \left[u_1 + \frac{u_3 - u_1}{\delta} z \right] dz = a_2 \frac{u_3 + u_1}{2},$$

and, from this expression, it follows (7) taking into account that $q_i = a_i u_i$, $i = 1, 3$.

Because of the hypothesis of linearity of profiles, the system of Equations (5)–(7) is linear in q_i and, so, explicit expressions are obtained for such variables. Solving this system, we obtain

$$q_1 = -b_3 \gamma, \quad q_2 = R - (b_1 - b_3) \gamma, \quad q_3 = b_1 \gamma \quad (8)$$

where

$$\gamma = \frac{2a_1 a_3 R}{a_1 b_1 (a_2 + 2a_3) - a_3 b_3 (a_2 + 2a_1)},$$

$$b_1 = \left(1 + \frac{a_2}{3a_1} \right) s_1 + \frac{a_2}{6a_1} s_3,$$

$$b_3 = \left(1 + \frac{a_2}{3a_3} \right) s_3 + \frac{a_2}{6a_3} s_1.$$

On the other hand, the equations to determine vertical water and salt fluxes between the three layers in any compartment n of the estuary are:

$$q_1(n-1) + q_{21}(n) = q_1(n) + q_{12}(n) \quad (9)$$

$$q_3(n-1) + q_{23}(n) = q_3(n) + q_{32}(n) \quad (10)$$

$$q_1(n-1) s_1(n-1) + q_{21}(n) \bar{s}_2(n) = q_1(n) s_1(n) + q_{12}(n) \bar{s}_1(n) \quad (11)$$

$$q_3(n-1) s_3(n-1) + q_{23}(n) \bar{s}_2(n) = q_3(n) s_3(n) + q_{32}(n) \bar{s}_3(n) \quad (12)$$

where the single subscripts have the same meaning as in the previous equations, and $q_i(n)$, $s_i(n)$ are equivalent to q_i , s_i from Equations (1) to (4), whereas $q_i(n-1)$, $s_i(n-1)$ refer to the beginning of the compartment (see Figure 3). The double subscript ij refers to the vertical flux from the i -layer to the j -layer. The numbering of the compartments is from the beginning of the wedge ($n=1$) to the mouth of the river ($n=N$), being $\bar{s}_i(n) = (s_i(n) + s_i(n-1))/2$. Equations (9) and (11) are, respectively, the salt and water continuity conditions for the upper layer, and (10) and (12) are the same conditions for the salt wedge layer.

Introducing the expressions of horizontal fluxes q_i given by (8) in the system of Equations (9)–(12) and solving it (again the system is linear), vertical fluxes are obtained for a given compartment n . These vertical fluxes are given by

$$q_{21}(n) = \frac{q_1(n) [s_1(n) - \bar{s}_1(n)] - q_1(n-1) [s_1(n-1) - \bar{s}_1(n)]}{\bar{s}_2(n) - \bar{s}_1(n)},$$

$$q_{12}(n) = \frac{q_1(n) [s_1(n) - \bar{s}_2(n)] - q_1(n-1) [s_1(n-1) - \bar{s}_2(n)]}{\bar{s}_2(n) - \bar{s}_1(n)},$$

$$q_{23}(n) = \frac{q_3(n) [s_3(n) - \bar{s}_3(n)] - q_3(n-1) [s_3(n-1) - \bar{s}_3(n)]}{\bar{s}_2(n) - \bar{s}_3(n)},$$

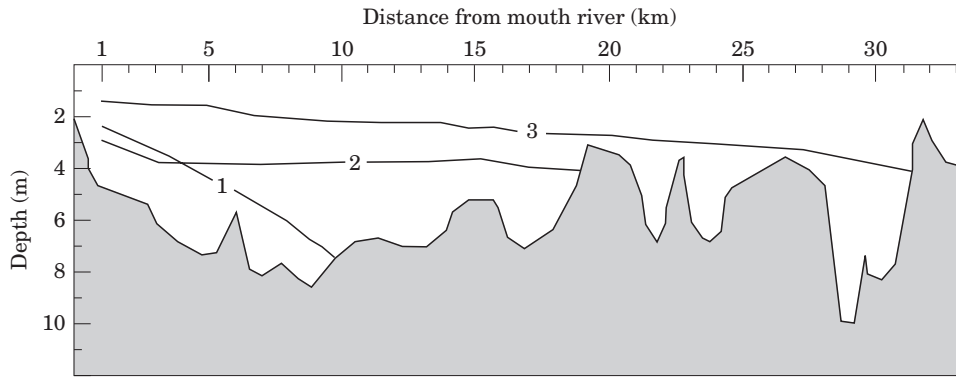


FIGURE 4. Salinity distribution in the Ebre estuary in three different surveys, representing the three most frequent steady positions of the salt wedge: (1) limit at 9.5 km from the mouth, (2) limit at 18 km from the mouth and (3) limit at 30 km, the maximum extent.

$$q_{32}(n) = \frac{q_3(n)[s_3(n) - \bar{s}_2(n)] - q_3(n-1)[s_3(n-1) - \bar{s}_2(n)]}{\bar{s}_2(n) - \bar{s}_3(n)},$$

Where $\bar{s}_2(n)$ is computed using the mean value of the salinity of the interface at each profile. These fluxes can be separated into *entrainment* from the lower layer to the interface, q_{32} , and from the interface to the upper layer, q_{21} , and *turbulent exchange* between the i -layer ($i=1, 3$) and the interface, i.e. the net fluxes $q_{21} - q_{12}$ and $q_{32} - q_{23}$, respectively (see Application of the model).

Finally, to take into account the boundary conditions of the estuary, the system of equations for each compartment has to be solved starting with the closest compartment to the upstream edge of the estuary. For the first compartment, $q_1(n-1)=R$, $q_3(n-1)=0$ and $s_1(n-1)=0$.

In more mixed estuaries, when a well defined interface layer is not noticeable, only two layers can be considered: the upper one moving to the sea and the lower one moving inland. In this case, the system of equations for horizontal fluxes becomes as:

$$\begin{aligned} q_1 s_1 + q_3 s_3 &= 0 \\ q_1 + q_3 &= R, \end{aligned}$$

which is an expression of Knudsen's Hydrographical Theorem. Similarly, the system of equations for vertical fluxes becomes as:

$$\begin{aligned} q_1(n-1) + q_{31}(n) &= q_1(n) + q_{13}(n) \\ q_1(n-1)s_1(n-1) + q_{31}(n)\bar{s}_3(n) &= q_1(n)s_1(n) + q_{13}(n)\bar{s}_1(n) \end{aligned}$$

Results

Physical structure of the estuary

The three most common steady positions of the salt wedge in the Ebre estuary are shown in Figure 4. Position 1 occurs when river discharge is in the range $300\text{--}400 \text{ m}^3 \text{ s}^{-1}$, just below the mean annual discharge. Position 2, which is the most frequent, occurs when the river discharge is in the range $100\text{--}300 \text{ m}^3 \text{ s}^{-1}$. Notice that the tip of the salt wedge is located close to a shallow area (Gràcia Island), at 18 km from the mouth. Position 3 occurs when river discharge is lower than $100 \text{ m}^3 \text{ s}^{-1}$, representing the maximum extent of the salt wedge (see Ibàñez, 1993 and Ibàñez *et al.*, 1997 for a detailed description of the salt wedge dynamics). Data from the survey carried out on 13 March 1989, with a steady river discharge of $60 \text{ m}^3 \text{ s}^{-1}$, is used to obtain numerical solutions of the model. The salinity contour plot obtained from profiles carried out every 2 km is shown in Figure 5. Notice the strong stratification along the whole estuary.

The profiles of salinity and velocity from a survey carried out on 30 May 1990, with a river discharge of $168 \text{ m}^3 \text{ s}^{-1}$, are shown in Figure 6. Notice again the strong salinity stratification, with a well defined interface layer 40–50 cm thick. If one compares the profiles of salinity and velocity, it can be seen that the stagnant point always occurs at the end of the interface. This means that almost the whole interface flows downstream, in the same direction as the upper layer.

Application of the model

Results of horizontal and vertical fluxes calculated by the model are shown in Table 1 for $R=60 \text{ m}^3 \text{ s}^{-1}$. Notice that the magnitude of q_3 decreases in the

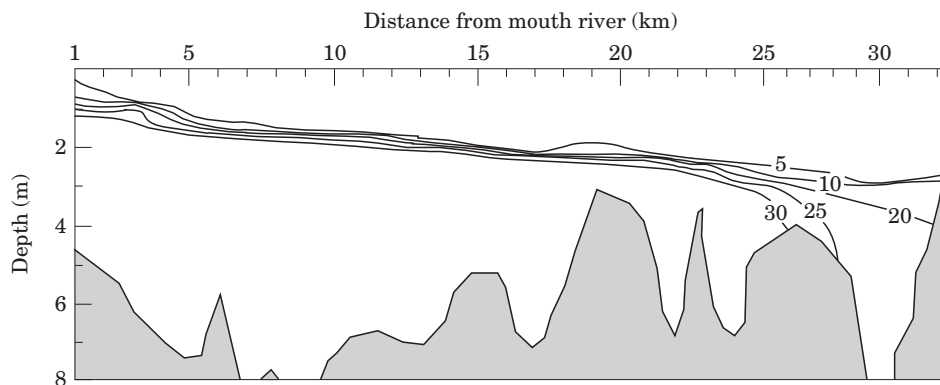


FIGURE 5. Salinity (g/l) contour plot along the Ebre estuary on 13 March 1989.

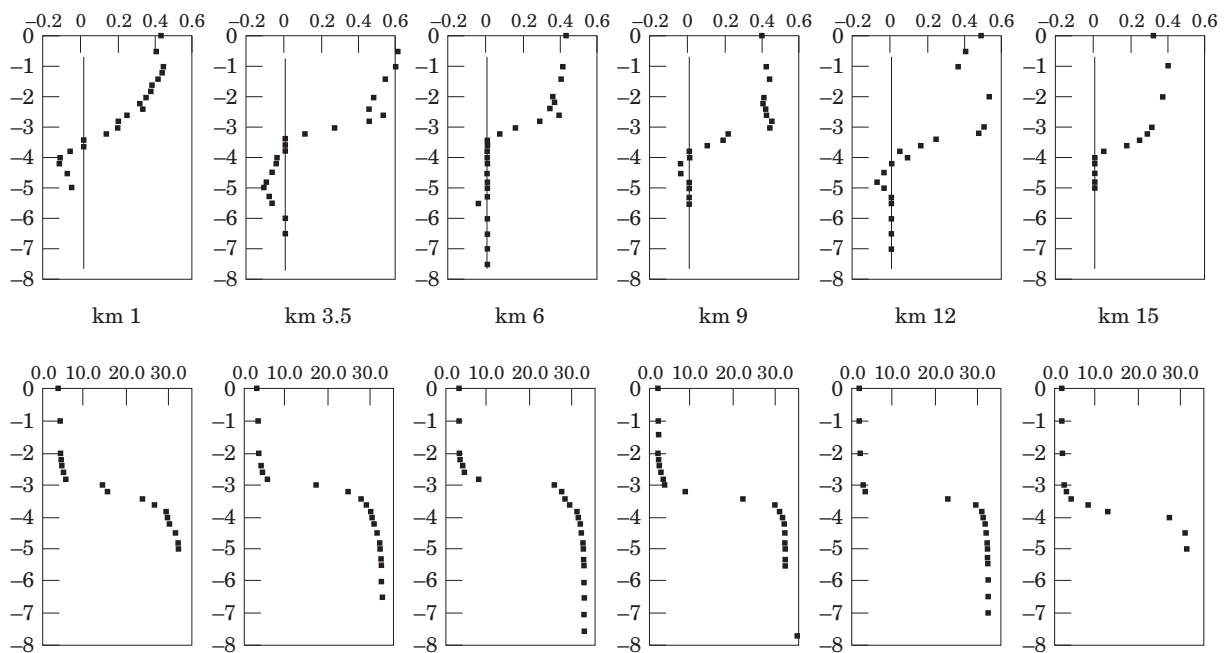


FIGURE 6. Velocity (m/s) and salinity (g/l) profiles along the Ebre estuary, on 30 May 1990.

upriver direction, as would be expected, but in one compartment (25–27 km) it has a significant increase of $0.5 \text{ m}^3 \text{ s}^{-1}$. The existence at the same compartment of a natural source of underground fresh water in the bed of the river, causing an input of water into the salt wedge and decreasing its salinity (Ibáñez, 1993), could explain the anomalous flux in the salt wedge predicted by the model. Assuming that the decrease of salinity in the salt wedge from 31.5 to 24.0 g/l was solely due to a source of underground pure fresh water (with no water fluxes from the interface and upper layers), which mixes with the water coming from the salt wedge, then the corresponding input of underground water would be $0.43 \text{ m}^3 \text{ s}^{-1}$, very close to the increase of flux pre-

dicted by the model. Since this local input of fresh water was not introduced as data, the model ‘solves’ this problem by producing a vertical flux of water of $0.5 \text{ m}^3 \text{ s}^{-1}$ from the upper (fresh water) layer to the salt wedge. Notice that there is no salinity increase in the upper layer at this compartment, so the vertical flow from the interface to the upper layer predicted by the model is zero. Then there is no physical reason to produce the vertical water flow from the upper layer to the salt wedge, because the pure entrainment of water to the salt wedge could only take place if the water velocity at the salt wedge was much larger than at the upper layer, and this is not the case.

The values of the vertical fluxes give information about entrainment and mixing processes between the

TABLE 1. Averaged salinity values in the upper (s_1) and lower (s_3) layers of the Ebre river estuary based on a survey carried out on 13 March 1989. The results of horizontal and vertical fluxes ($m^3 s^{-1}$) computed by running the model (with $R=60$ and cross sectional areas given in Table 3) are shown in columns 4 to 10. In last four columns the values of Ie_{ij} , the index of entrainment defined in *Application of the model*, the Richardson number at the interface (Ri), and K_z , the eddy diffusion coefficient ($cm^2 s^{-1}$), are also shown, respectively

km	s_1	s_3	q_1	q_2	q_3	q_{12}	q_{21}	q_{32}	q_{23}	Ie_{21}	Ie_{32}	Ri	K_z
31	0.0	0.0	60.0	—	—	—	—	—	—	—	—	—	—
29	0.08	23.9	58.5	2.5	-1.0	1.9	0.4	1.2	0.2	-0.63	0.68	4.75	0.0106
27	0.60	24.0	59.8	2.5	-2.3	1.4	2.6	1.3	0.0	0.32	0.98	7.08	0.0097
25	0.60	31.5	59.3	2.5	-1.8	0.5	0.0	0.7	1.1	-1.00	-0.26	13.16	-0.0041
23	0.68	33.1	59.2	3.0	-2.2	0.4	0.3	0.5	0.2	-0.16	0.43	7.52	0.0021
21	0.75	33.9	58.9	3.5	-2.4	0.5	0.2	0.3	0.1	-0.33	0.51	9.06	0.0011
19	0.82	34.3	59.0	3.3	-2.3	0.1	0.2	0.0	0.1	0.28	-0.67	12.79	-0.0004
17	0.83	34.8	59.0	3.5	-2.5	0.0	0.1	0.3	0.1	0.25	0.58	3.70	0.0019
15	0.88	34.8	58.8	4.1	-2.9	0.4	0.2	0.4	0.0	-0.39	1.00	4.01	0.0033
13	1.18	34.8	59.3	4.1	-3.3	0.6	1.0	0.5	0.0	0.28	1.00	10.50	0.0022
11	1.53	34.8	59.5	4.9	-4.3	1.1	1.3	1.0	0.0	0.14	1.00	3.05	0.0076
9	1.88	34.8	59.9	5.2	-5.1	0.8	1.3	0.7	0.0	0.22	1.00	2.81	0.0052
7	2.27	34.8	60.4	5.5	-5.9	0.9	1.5	0.9	0.0	0.23	1.00	1.85	0.0077
5	2.40	34.8	60.4	6.0	-6.4	0.5	0.5	0.4	0.0	-0.05	1.00	2.04	0.0030
3	2.89	34.8	59.1	9.3	-8.5	3.1	1.8	2.1	0.0	-0.26	1.00	0.66	0.0178
1	4.84	34.8	60.3	13.6	-13.9	6.4	7.5	5.5	0.0	0.08	1.00	1.32	0.0414

three layers. The differences $q_{21}-q_{12}$ and $q_{32}-q_{23}$ are the net vertical fluxes and they indicate the degree of entrainment. When q_{23} approaches 0, there is pure entrainment from the salt wedge to the interface, as happens in most of the estuary. The higher q_{32} , the higher is the entrainment, which is maximum near the mouth of the Ebre estuary. The net flux between the salt wedge and the interface divided by the surface area between them gives the entrainment velocity u_e . For the studied case, its mean value was $u_e=2.21 \times 10^{-4} cm s^{-1}$, with a maximum of $1.03 \times 10^{-3} cm s^{-1}$ at the compartment closest to the mouth. These values are one order of magnitude lower than those found in the Duwamish salt wedge estuary (Partch & Smith, 1978), likely due to a higher tidal mixing in the latter.

On the other hand, the higher and more similar the values of q_{12} and q_{21} or q_{23} and q_{32} , the stronger and more turbulent is the mixing between the upper layer and the interface or between the interface and the salt wedge, respectively. In general, the results show that the vertical mixing is more intense and turbulent between the interface and the upper layer than between the interface and the salt wedge. The relative magnitude of the processes of entrainment and vertical mixing can be quantified by means of the following indexes of entrainment:

$$Ie_{32} = (q_{32} - q_{23}) / (q_{32} + q_{23})$$

$$Ie_{21} = (q_{21} - q_{12}) / (q_{21} + q_{12})$$

Table 1 lists values of these indexes computed from the results of the vertical fluxes.

The indexes ranges from -1 to 1, indicating pure entrainment from the layer 1 to 2 when $Ie_{21} = -1$, or from 2 to 3 when $Ie_{32} = -1$, and in converse sense when $Ie_{21} = 1$ or $Ie_{32} = 1$. The more the values approach to 0, the more turbulent is the vertical mixing and the less the entrainment. The mixing between the upper layer and the interface is turbulent in most of the estuary, whereas between the interface and the salt wedge it is less turbulent (upper half) or not turbulent (lower half). However, in stratified estuaries with strong tides, as the Fraser estuary, entrainment from the interface to the lower layer has been reported (Geyer, 1985).

While alternation of positive and negative values of Ie_{21} along the estuary reflects a turbulent vertical mixing between the interface and the upper layer, the almost permanent positivity of Ie_{32} indicates a predominance of entrainment from the salt wedge to the interface. The negative values of Ie_{32} at 19–21 km and 25–27 km are probably due to the reduction of the cross section of the salt wedge (cf. Table 3) and hence, the increase of the water velocity in this layer causing a higher vertical flux between the interface and the salt wedge. Moreover, the increase of the width in the upper layer and the decrease of depth in the lower layer also favour the diffusive vertical mixing by winds and internal waves. Finally, notice that the decrease of salinity at 19–21 km of the salt wedge is much lower

TABLE 2. Results of advective water fluxes ($\text{m}^3 \text{s}^{-1}$) in the salt wedge of the Ebre estuary (13 March 1989), using three different methods: the three-layer model, the Knudsen two-layer model considering the division of the interface at the stagnant point ($K_{u=0}$), and the Knudsen's two-layer model splitting up the interface in two equal parts (K_{half}). % refers to the degree of overestimate or underestimate relative to the three-layer model

km	3 layer	$K_{u=0}$	%	K_{half}	%
1	-13.9	-21.6	55.4	-13.5	-2.9
3	-8.5	-14.1	65.9	-7.9	-7.1
5	-6.4	-10.0	56.2	-6.1	-4.7
7	-6.0	-9.3	55.0	-5.7	-5.0
9	-5.1	-8.3	62.7	-4.8	-5.9
11	-4.3	-7.3	69.8	-4.1	-4.7
13	-3.3	-5.8	75.8	-3.3	0.0
15	-2.9	-5.4	86.2	-2.6	-10.3
17	-2.5	-4.6	84.0	-2.5	0.0
19	-2.3	-4.3	87.0	-2.6	13.0
21	-2.4	-4.4	83.3	-2.4	0.0
23	-2.2	-4.0	81.8	-2.1	-4.5
25	-1.8	-3.4	88.9	-2.1	16.7
27	-2.3	-3.8	65.2	-2.3	0.0
29	-1.0	-2.6	160.0	-0.8	-20.0

than the one at 25–27 km, where an input of underground fresh water also takes place (see above).

The Richardson number at the interface (Ri) ranges from 0.66 at 3 km to 13.16 at 25 km (see Table 1). The values of the eddy diffusion coefficient (K_z) range from $-0.0004 \text{ cm}^2 \text{ s}^{-1}$ at 19–21 km to $0.0414 \text{ cm}^2 \text{ s}^{-1}$ at 1–3 km. The highest values of Ri occur in the upper estuary and, in general, Ri decreases towards the mouth. However, there are three noticeable maxima of Ri at 13, 19 and 25 km which are coincident with minimum values of the velocity of the upper layer (in turn due to an increase of the cross section, see Table 3). The maxima of Ri are also coincident with minimum values of K_z at the pycnocline, which, in general terms, shows an inverse correlation with Ri.

The results of different estimates of the water fluxes along the salt wedge (q_3), comparing the values produced by the three-layer model (data from Table 1) and the results produced by the two-layer Knudsen's model, are shown in Table 2. The correct criteria to divide the water column into two layers has to be the stagnant point, which divides the part of the water column which flows downstream (upper layer) and the part which flows upstream (lower layer). Remember that in highly stratified estuaries the stagnant point is placed very close to the lower edge of the interface, because water velocities at the lower layer are very small compared to those of the upper layer. For the studied case, the Knudsen's model produces an overestimate of advective water fluxes at the salt wedge

TABLE 3. Ebre river cross sectional areas (in m^2) of the layers used to compute the fluxes

km	a_1	a_2	a_3
1	218	106	730
3	163	53	826
5	293	60	806
7	279	53	640
9	339	61	699
11	347	59	715
13	671	101	422
15	386	55	707
17	394	51	190
19	798	109	176
21	634	83	240
23	578	64	237
25	738	78	121
27	664	60	290
29	493	42	488

which ranges from 55 to 160%. The results of applying the Knudsen's model incorporating the upper half of the interface to the upper layer and the lower half of the lower layer are shown in the last column. Notice that the results are more similar to the results predicted by the three layer model, although there is a small underestimate.

Discussion

The model presented gives a better, physically based, estimate of advective fluxes in highly stratified

estuaries than Knudsen's two-layer model. Since the interface is not considered as a separate layer in the Knudsen's model, it cannot incorporate the particularities of salt transport at this layer. In fact, the application of the two-layer Knudsen's model to highly stratified estuaries, where a defined interface with opposite linear profiles of salinity and velocity exists, must always produce an overestimate of advective fluxes in the estuary.

The possibility of determining horizontal and vertical fluxes of water and salt in a given compartment allows the study of the advective processes and mixing between the three layers along the estuary, and can be used to investigate factors affecting these processes, such as local changes in the dimensions of the estuary. Another possibility is using the model to assess nutrient fluxes in highly stratified estuaries, or as the base for modelling other processes like pollutant dispersal or oxygen budgets. This is possible in estuaries where advective processes prevail over the diffusive ones, say, highly stratified estuaries with low tidal range, like those from the Mediterranean and the Gulf of Mexico.

It has to be noted that empirical validation in terms of tidally averaged velocities of the upper and lower layers is not possible with present data because velocity profiles are instantaneous. However, we want to stress that as the Ebre estuary is located in a microtidal sea, the time-independent approach presented in this paper is appropriate. On the other hand, the results of salt transport in the salt wedge are quite similar to those obtained with the Knudsen's models when the division of both layers is located at the middle point of the interface. Nevertheless, from a modelling point of view, there is no physical reason (in terms of water and salt transport) to use such criterion of division of the interface.

Acknowledgements

We would like to thank Frank Torre from the Laboratoire d'Ecologie des Systèmes Fluviaux (Arles,

France) for helping us; John W. Day Jr., from the Department of Oceanography and Coastal Sciences, Louisiana State University, for reviewing the manuscript; and W. R. Geyer from the Woods Hole Oceanographic Institution, who suggested some ideas about the construction of the model. C.I. and N.P. thank also the Ministerio de Educación y Ciencia of the Spanish Government, which partially supported this research, as well as the EC Environment Research Program 'Climatology and Natural Hazards': MED-DELT, Impact of Climatic Change on Northwestern Mediterranean Deltas (contract EV5V-CT94-0465).

References

- Geyer, W. R. 1985 The time-dependent dynamics of a salt wedge. Ph.D. Thesis, University of Washington, 199 p.
- Geyer, W. R. & Smith, J. D. 1987 Shear instability in a highly stratified estuary. *Journal of Physical Oceanography* **17**, 1668–1679.
- Geyer, W. R. & Farmer, D. M. 1989 Tide induced variation of the dynamics of a salt wedge estuary. *Journal of Physical Oceanography* **19**, 1060–1072.
- Guillén, J. 1992 Dinámica y balance sedimentario en los ambientes fluvial y litoral del Delta del Ebro. Ph.D. Thesis, Universitat Politècnica de Catalunya. (In Spanish). Barcelona, Spain.
- Ibàñez, C. 1993 Dinàmica hidrològica i funcionament ecològic del tram estuari del riu Ebre. Ph.D. Thesis, University of Barcelona, 198 p. (in Catalan). Barcelona, Spain.
- Ibàñez, C., Rodríguez-Capítulo, A. & Prat, N. 1995 The combined impacts of river regulation and eutrophication on the dynamics of the salt wedge and the ecology of the lower Ebro river. In *The Ecological Basis for River Management* (Harper, D. M. & Ferguson, A., eds). John Wiley & Sons, Chichester, England.
- Ibàñez, C., Pont, D. & Prat, N. 1997 Characterization of the Ebre and Rhone estuaries: a basis for defining and classifying salt-wedge estuaries. *Limnology and Oceanography* **42**, 89–101.
- Keulegan, H. G. 1966 The mechanism of an arrested saline wedge. *Estuary and Coastline Hydrodynamics*. New York.
- Muñoz, I. & Prat, N. 1989 Effects of river regulation on the lower Ebro river. *Regulated Rivers* **3**, 345–354.
- Partch, E. N. & Smith, J. D. 1978 Time dependent mixing in a salt wedge estuary. *Estuarine and Coastal Marine Sciences* **6**, 3–19.
- Rattray, M. & Mitsuda, E. 1974 Theoretical analysis of conditions in a salt wedge. *Estuarine and Coastal Marine Sciences* **2**, 375–394.
- Wright, L. D. & Coleman, J. M. 1971 Effluent expansion and interfacial mixing in the presence of a salt wedge, Mississippi River Delta. *Journal of Geophysical Research* **36**, 8649–8661.